Radial spin Hall effect of light

Weixing Shu,[1,2] Yougang Ke,[1] Yachao Liu,[1] Xiaohui Ling,[1] Hailu Luo,[1] and Xiaobo Yin[2,*]

[1]*Key Laboratory for Micro-/Nano-Optoelectronic Devices of Ministry of Education, College of Computer Science and Electronic Engineering, Hunan University, Changsha 410082, China*

[2]*Department of Mechanical Engineering, University of Colorado, Boulder, Colorado 80309, USA*

We propose and realize a radial spin Hall effect (SHE) of light by using a dielectric metasurface. The metasurface with radially varying optical axes introduces a Pancharatnam–Berry (PB) geometrical phase to the incident light. The spatial gradient of PB phase accounts for a shift in the momentum space and thus leads the light to split radially into two concentric rays with opposite spin in the position space, which is called a radial SHE. Further experiments verify that the magnitude of the splitting increases with the rotation rate of the optical-axis orientation and the propagation distance, thereby allowing for macroscopic observation of the SHE. We also find that the phase of the incident light influences the profiles of the two split rays, while the polarization determines their intensities. The results provide methods to tune the SHE of light by engineering metasurfaces and modulating the incident light, and this radial SHE may be extrapolated to other physical systems.

I. INTRODUCTION

In the past few years the spin Hall effect (SHE) of light was intensively studied owing to the universality of the underlying physics and potential applications in diverse physical systems [1–12]. The SHE manifests itself as the spin-dependent transverse shift of the photon trajectory due to the spin-orbit interaction (SOI) of light [13–15], while warranting the conservation of angular momentum [16,17]. It also means the spin-dependent splitting (SDS) of a ray of mixed polarizations into two circularly polarized rays [4]. Analogous to the electrical SHE, the demonstration of photonic SHE [3,4] has great scientific value and offers wide-ranging opportunities for new physics and unique applications. Based on the SHE a new area of research, spinoptics, promises to be developed [4,14]. The SHE has thus far been applied to probing nanodisplacement [18] and characterizing nanostructures [19,20].

In the previously reported SHE, a common feature is that the SDS is lateral with two split rays lying on opposite sides of the otherwise beam centroid [5,14,15]. Here, we report a unique SHE with a radial SDS that brings about two concentric rays by a dielectric metasurface in the visible regime. As a two-dimensional (2D) subwavelength structure, the metasurface allows for accurate control of the phase and polarization of the wave [21,22]. It has been used to control reflection and refraction [23], to manipulate the spin or orbital angular momentum of photons [23–25], and to enhance the SHE of light [7,9,26–28]. Such an unprecedented degree of freedom in controlling SOI naturally inspires us to search for new SDSs or SHEs.

In particular, we implement a radial SDS by an inhomogeneous anisotropic metasurface that has a periodically varying optical-axis distribution. Such a metasurface is fabricated via femtosecond-laser writing of spatially varying nanogrooves in a fused silica sample [29,30]. Through the metasurface the polarization of light will be changed, thereby imparting

a Pancharatnam–Berry (PB) geometrical phase onto the light [31–34]. The gradient of PB phase accounts for a shift in momentum space [5,7,35] and then induces a radial SDS in position space. This is in contrast with the conventional SHE [5,15] including the azimuthal SHE [14,36] and the geometric SHE [6,11]. We call this effect a radial SHE.

Different from the previous SHE where the intensity of the light beam does not split [37–40], the present SHE manifests itself as the simultaneous SDSs of spin and intensity due to the asymmetrical distribution of metasurface elements [26,28]. Moreover, the SHE is tunable: its magnitude can be changed by tailoring the optical-axis orientation in the metasurface; the position and the intensity of the resulting ray can be changed by modulating the phase and polarization of the incident light, respectively. The results are further validated by experiments. Our results add another member to the SHE of light and provide flexible and efficient ways to generate and control radial-variant vector fields. Such a radial SHE may be extended to other physical systems.

II. THEORETICAL FORMULATION

The SOI of light [13] describes the transverse nature of waves, which indicates the mutual interplay of polarization (spin) and trajectory (orbital angular momentum) of light. According to the SOI, the SHE of light can be classified into two types [7,14]: (i) The first type results from the change of the trajectory of light in inhomogeneous but locally isotropic media or at optical interfaces [1–4]. (ii) The second type originates from the change of polarization of light in an inhomogeneous anisotropic medium [5,7,9]. The first type of SHE is often rather tiny because the SOI in ordinary optical media is weak [15]. The resultant SDS is typically on the subwavelength scales and its detection has to resort to a coherent enhancement technique based on quantum weak measurements [3]. In contrast, the second SHE can be manipulated to obtain giant SDS [5,7,9]. Therein the SOI can be enhanced considerably by properly designed structures, such as subwavelength gratings [33,34], liquid crystal q plates [41], plasmonic chains [7], and dielectric [29,30] or

*xiaobo.yin@colorado.edu

plasmonic [27,37,38] metasurfaces. In the present work, we follow the mechanism of the second type of SHE to realize a macroscopic SDS in the visible regime by a dielectric metasurface.

Let us first consider a half-wave plate (HWP) that possesses an inhomogeneous distribution of the optical axis. The optical-axis orientation forms an angle against the radial direction $\hat{r}$:

$$\alpha = \Omega r + \alpha_0. \qquad (1)$$

Here, $\Omega = \pi/d$ is the rotation rate of the optical axis with d being the period, r is the radial coordinate, and α_0 specifies the orientation at $r = 0$. In Eq. (1) we assume α to be linearly dependent on r for simplicity.

The SOI and SHE of light were first introduced by using the so-called Berry connection and Berry curvature as in the SHE of electrons [1,4]. But now they are more usually described by wave optics which leads to intuitive understanding and simple calculations [2,7,13]. Here we follow the latter method and adopt a Jones formalism to analyze the SOI induced by the inhomogeneous anisotropic medium [34,39]. The Jones matrix M of the HWP can be written as [14,41]

$$M = \begin{pmatrix} \cos 2\alpha & \sin 2\alpha \\ \sin 2\alpha & -\cos 2\alpha \end{pmatrix}. \qquad (2)$$

Without loss of generality, a homogeneous elliptically polarized light is considered to impinge on the slab at normal incidence. It can be geometrically represented by a point on the Poincaré sphere [Fig. 1(a)] [42,43] and algebraically described in terms of the polar angle θ and the azimuth angle φ on the sphere [44,45]:

$$|E_{\text{in}}\rangle = \cos\left(\frac{\theta}{2}\right)e^{-i\frac{\varphi}{2}}|R\rangle + \sin\left(\frac{\theta}{2}\right)e^{i\frac{\varphi}{2}}|L\rangle, \qquad (3)$$

where $|R\rangle = (\hat{x} + i\hat{y})/\sqrt{2}$ and $|L\rangle = (\hat{x} - i\hat{y})/\sqrt{2}$ represent the right- and left-circular-polarization states, respectively.
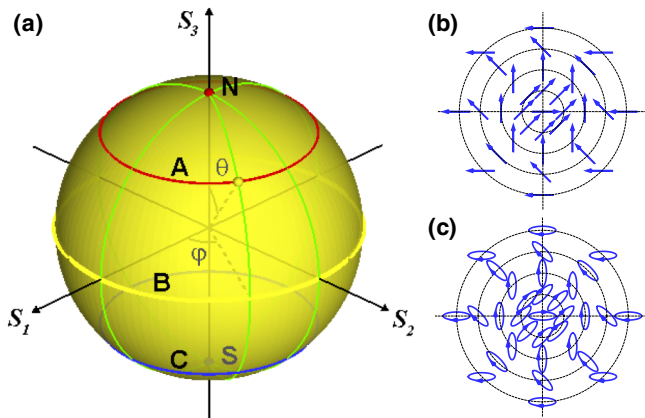
FIG. 1. (a) Poincaré sphere. Equi-latitude states on the Poincaré sphere constitute five types of space-variant polarization distributions in the radial direction for the CV beams discussed in the present work. The five consist of linear, right (left) elliptical, and right (left) circular-polarization states on the equator B, the circle A (C), and the north (south) pole N (S), respectively. Panels (b) and (c) show schematic pictures of two typical radial-variant polarizations, respectively composed of polarization states on B and A in panel (a).

Through the HWP the resulting light is

$$|E_{\text{out}}\rangle = \cos\left(\frac{\theta}{2}\right)e^{i(2\alpha - \frac{\varphi}{2})}|L\rangle + \sin\left(\frac{\theta}{2}\right)e^{-i(2\alpha - \frac{\varphi}{2})}|R\rangle. \qquad (4)$$

For spatially varying α, such a superposition of orthogonal circular-polarization components forms a radial-variant polarization beam with cylindrical symmetry [Fig. 1(c)], i.e., a cylindrical vector (CV) beam [46–48]. A simple case is that, if the incident light is linearly polarized ($\theta = \pi/2$), $|E_{\text{in}}\rangle = [\cos\frac{\varphi}{2}, \sin\frac{\varphi}{2}]$, the emerging light has a radial-variant linear polarization [47]

$$|E_{\text{out}}\rangle = \begin{bmatrix} \cos\left(2\alpha - \frac{\varphi}{2}\right) \\ \sin\left(2\alpha - \frac{\varphi}{2}\right) \end{bmatrix}, \qquad (5)$$

as shown in Fig. 1(b).

A comparison of Eq. (4) with Eq. (3) shows that the incident $|R\rangle$ transforms into the output $|L\rangle$ carrying an additional phase

$$\Phi_{PB} = 2\sigma\alpha, \qquad (6)$$

and vice versa. Here, $\sigma = \pm 1$ represent the spin of $|R\rangle$ and $|L\rangle$, respectively. This phase is just the PB phase [33,34,41]. It depends on location for Eq. (1) and its gradient amounts to a spin-dependent momentum deviation [5,7]

$$\Delta\mathbf{k} = -\nabla\Phi_{PB}. \qquad (7)$$

This shift will deflect the wave vector by an angle $\Delta\mathbf{k}/k_0$ where k_0 is the wave number in free space [14,49]. Consequently the wavefront is modified and the wave centroid undergoes a spatial shift $z\Delta\mathbf{k}/k_0$ [28,35],

$$\Delta\mathbf{r} = -\sigma\frac{2\Omega}{k_0}z\hat{r} = -\sigma\frac{\lambda}{d}z\hat{r}, \qquad (8)$$

after propagating a distance z.

It can be concluded from Eq. (8) that (i) an incident elliptically polarized light is split by the plate into $|R\rangle$ and $|L\rangle$ which shift oppositely in the radial direction. This shift of trajectory equals the gradient of the PB phase arising from the change of polarization (spin). Therefore, it demonstrates the SOI of light introduced by the space-variant anisotropic elements and can be regarded as an extrinsic SHE [14]. This SHE manifests itself as a unique radial SDS, in contrast with the lateral SDS in the conventional SHE [5,15] including the azimuthal SHE [14,36] and the geometric SHE [6,11]. For this reason, we may call this effect a radial SHE. (ii) The shift is proportional to the rotation rate of optical axis Ω, so the SHE can be controlled by engineering the rotation period of the optical axis in the inhomogeneous HWP. (iii) The shift also increases with z, enabling the direct observation of the radial SDS. (iv) This shift is independent of θ in Eq. (4), i.e., the shape of the incident polarization ellipse.

III. EXPERIMENTAL IMPLEMENTATION

To verify the radial SHE, we designed a metasurface with optical axes periodically varying in the radial direction, as in Eq. (1). Such a metamaterial was fabricated by etching continuously varying grooves in a fused silica sample by using a femtosecond laser [29,30]. The resulting self-assembled nanogratings produce a form birefringence with the slow and fast optical axes parallel and perpendicular to the grating
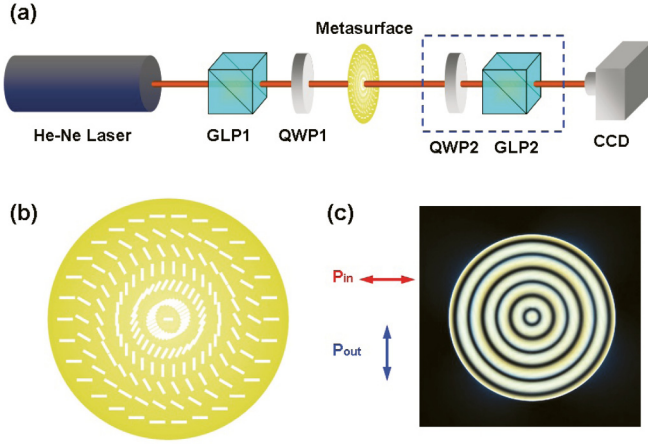
FIG. 2. Experimental setup to generate CV beams with radial-variant polarizations and to observe the radial SHE. (a) A He-Ne laser (632.8 nm, 17 mW, Thorlabs HNL210L-EC) outputs a linearly polarized Gaussian beam. GLP stand for Glan laser polarizer, QWP stands for quarter-wave plate, and CCD stands for charge-coupled device (Coherent LaserCam HR). (b) Schematic illustration of the local optical axes (slow axes) in the metasurface. (c) Cross-polarization intensity picture of the metasurface. The input and output polarizations are denoted by the arrows on the left.

grooves, respectively. By controlling the etched depth of the grooves, a retardation of π can be achieved. Because the periodicity of nanogratings is sufficiently smaller than the illumination beam's wavelength, the metasurface effectively behaves as an inhomogeneous HWP needed (Altechna). Finally the polariscopic analysis was carried out [49] and the result is shown in Fig. 2(c), which proves that the metasurface has a satisfactory radial-variant distribution of the optical axes.

We built an experiment setup to validate the radial SHE [Fig. 2(a)]. A fundamental Gaussian beam with a 2.1 mm waist from a collimated He-Ne laser was properly polarized by orienting a polarizer (GLP1) and a quarter-wave plate (QWP1), and then was sent through the metasurface. The output beam was recorded by a CCD. Another quarter-wave plate (QWP2) and a polarizer (GLP2) were inserted to measure the Stokes parameters of the resulting beam.

A. Incidence of a solid beam

We illuminated the metasurface with a linearly polarized Gaussian beam to generate the vector field, as in Eq. (5). The output transverse intensity is shown in Fig. 3(a). Obviously, the incident beam is split into one centroid and the other concentric ring. At the same time, the Stokes parameters [42,43] were measured to analyze the output polarization state. The first Stokes parameter S_0 is just the intensity of the output beam without QWP2 and GLP2. Combing QWP2 and GLP2, we get the parameters

$$S_1 = I(0°,0°) - I(90°,90°), \qquad (9)$$

$$S_2 = I(45°,45°) - I(135°,135°), \qquad (10)$$

$$S_3 = I(-45°,0°) - I(45°,0°). \qquad (11)$$
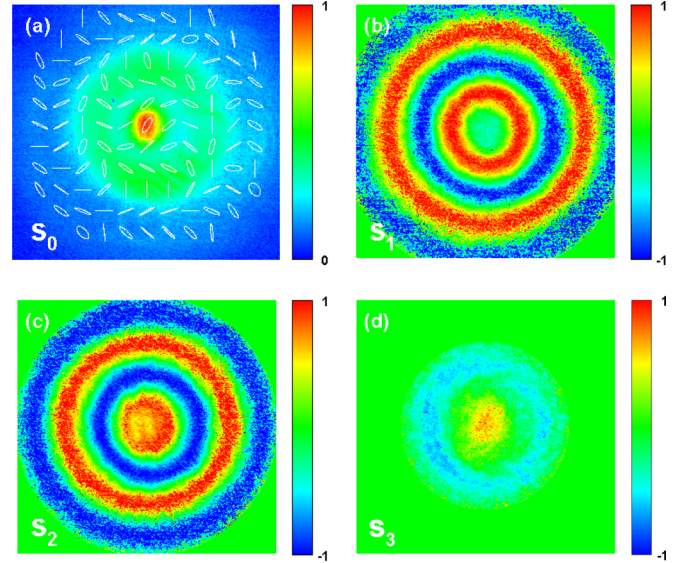
FIG. 3. The Stokes parameters experimentally measured at $z = 10$ cm for an incident linearly polarized Gaussian beam. According to S_0–S_3 in panels (a)–(d) the polarization state is retrieved, as shown in panel (a).

Here, $I(\alpha,\beta)$ represents the intensity recorded by CCD when the optical axis of QWP2 stays with α against the x axis and the polarization direction of GLP2 is β with respect to the same x axis.

The results of the normalized Stokes parameters $s_i = S_i/S_0$ ($i = 1,2,3$) are given in Figs. 3(b)–3(d). We know that s_1 reflects the tendency of polarization in the x ($s_1 = 1$) or $y(s_1 = -1)$ direction, s_2 implies the tendency of polarization in 45° ($s_2 = 1$) or $-45°$ ($s_2 = -1$) against the x direction, and s_3 reveals the degree of the right- ($s_3 = 1$) or left-handed ($s_3 = -1$) circular polarization. s_1 and s_2 in Figs. 3(b) and 3(c) indicate clearly the radial variation of polarization. s_3 in Fig. 3(d) proves that the incident linear polarization is split into two parts: the $|R\rangle$ centroid and the $|L\rangle$ ring. Figures 3(a) and 3(d) verify that the simultaneous SDS of the intensity and spin occur as expected. This is the radial SHE.

The Stokes parameters are then employed to retrieve the polarization state [50] according to the relationship between the formers and the latter [42,43]:

$$S_1 = S_0 \sin\theta \cos\varphi, \qquad (12)$$

$$S_2 = S_0 \sin\theta \sin\varphi, \qquad (13)$$

$$S_3 = S_0 \cos\theta. \qquad (14)$$

The retrieved results are illustrated in Fig. 3(a), which reveals again the tendency of radial change of polarization. Note that the appearance of polarization ellipses may result from either experimental or calculation errors. The results verify that the metasurface functions right as the inhomogeneous HWP required to produce the radial-variant polarization.

Next we studied the radial shift Δr of the resultant beams during propagation. The most intuitive and direct method to characterize the spin-dependent shift is to measure the
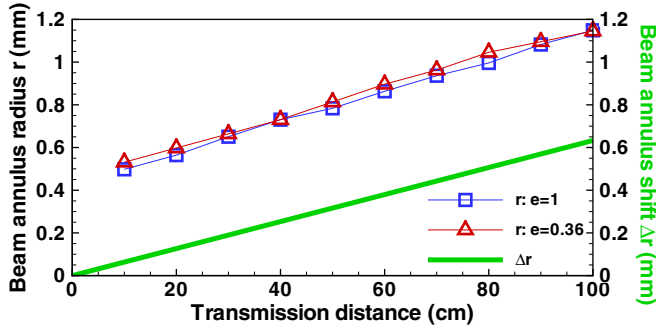
FIG. 4. Radial spin-dependent shift for an incident Gaussian beam. The solid line is the theoretical result of the radial shift for a metasurface with the optical-axis- variation period $d = 1000$ μm. Two groups of discrete points are the experimental results for the radii of left-circularly-polarized rings corresponding to the incidence of circular and elliptical polarizations with the ellipticity $e = 1$ and $e = 0.36$, respectively.

intensity center of the resultant beam minus that of the incident beam [3–5]. We first measured the intensity of the inner beam for different propagation distance z. We found that the centroid evolves from a Gaussian-like distribution of intensity near the exit surface $z = 10$ cm into a Bessel-like distribution at $z = 100$ cm (the results were not shown here). Since the inner beam is still solid as the incident beam, there is no radial shift between their intensity centers if using the common method mentioned above. We also found that the inner beam is much thinner than the incident Gaussian beam at the same position z. This result can be exploited to collimate beams [51], generate subwavelength beams [52,53], and realize subdiffraction focusing [54]. However, the relation of the spin-dependent shift with the beam width is not as intuitive or simple as that with the intensity center [15] because it involves complicated integrals, so it is difficult to calculate the analytical result of the exit beam. For this reason it has not yet been used to calculate the SDS [14].

Alternatively, we experimentally measured the radius of the outer ring at different transmission distance z. For simplicity, we chose a $|R\rangle$ light as the incident light. Through the metasurface it changes into an $|L\rangle$ single ring, for which the radius was measured, as shown by square symbols in Fig. 4. One can see that (i) the measured ring radii r increase linearly with z. They approximately lie on a straight line with the same slope as the theoretical shift Δr. (ii) The ring radius r is larger than Δr at a given z by a constant amount. This is because the initial radius r_0 of the ring at $z = 0$ is nonzero, akin to vortex beams [55]. But we did not measure r_0 because the dimensions of the CCD prohibit it from approaching the exit face of the metasurface, i.e. $z = 0$. If r_0 were measured, the result $r - r_0$ would agree with Δr.

Furthermore, we changed the incident light into an elliptical polarization (the ellipticity $e = 0.36$) and measured the radius of the resultant ring again. The results are denoted by triangular symbols in Fig. 4. By comparison, we find that the resultant ring exhibits the same radial shift as that of the $|R\rangle$ incidence. Obviously, the magnitude of SDS is independent of the incident polarization. It increases with propagation distance and the rotation rate of the optical-axis orientation. Therefore,
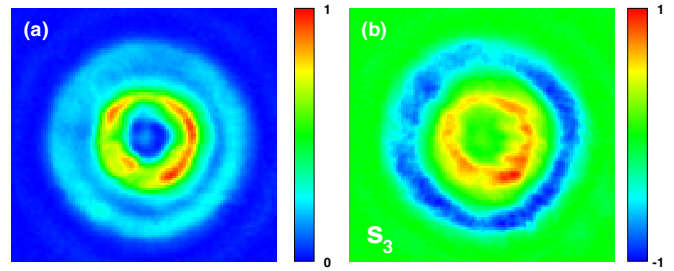
FIG. 5. Radial SHE for an incident linearly polarized vortex beam. Panels (a) and (b) show the transverse intensity and the Stokes parameter S_3 of the resulting beam measured at $z = 50$ cm away from the metasurface, respectively.

the experimental results validate the theoretical predications of Eq. (8).

B. Incidence of a vortex beam

As shown above, a solid beam is split into two beams: one hollow beam whose shift is just the radius of the ring and one solid beam on the axis whose shift is difficult to be measured. In order to measure both shifts unambiguously, we changed the incident light into a vortex beam with an off-axis intensity [55]. This hollow beam is produced by a spatial light modulator (SLM) which enables a Gaussian beam to carry a helical phase $\exp(il\phi)$ [56] before it impinges onto GLP1 in Fig. 2(a).

First, we measured the transverse intensity of the output beam emerging from the metasurface at a given transmission
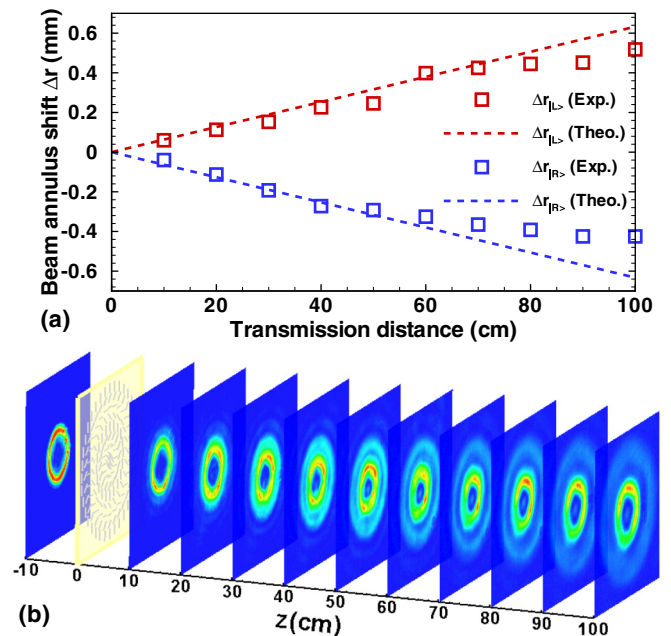
FIG. 6. (a) The theoretical and experimental results of the radial spin-dependent shifts for the incidence of vortex beam. $\Delta r_{|R\rangle}$ and $\Delta r_{|L\rangle}$ represent the shifts of the exit $|R\rangle$ and $|L\rangle$ hollow beams, respectively. (b) The process of the radial SHE. Shown are the transverse intensities of the beam measured at different transmission distances. The yellow plate denotes the metasurface.
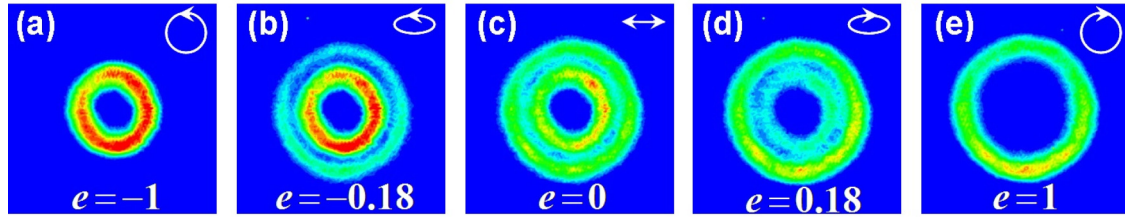
FIG. 7. Asymmetric spin-dependent splitting of intensity for incident elliptically polarized vortex beams. (a)–(e) Intensities recorded by the CCD for incident beams with $e = -1$, -0.18, 0, 0.18, 1, respectively. e represents the ellipticity of the incident polarization ellipse sketched on the upper right. The observation plane is located 40 cm away from the metasurface.

distance. The result for $l = 4$ and $z = 50$ cm is presented in Fig. 5(a), which displays two split rings of intensity. At the same time, we measured the Stokes parameter S_3 in order to examine the distribution of spin. The result in Fig. 5(b) shows that the vortex beam is split into two concentric hollow beams with opposite circular polarizations. It follows from Fig. 5 that the intensity and the spin are split simultaneously. Comparing Figs. 5(a) and 5(b) with Figs. 3(a) and 3(d), respectively, we see that the radial SDS is different between a vortex beam and a solid one. This means that the SHE can be tuned by the phase of the incident light. In addition, the position of split rings can be affected by the topological charge l. The larger the charge l, the larger the radius of the vortex beam [55,56] and thus the larger the radii of the resulting rings.

Second, we investigated the radial shifts of the split beams with different spins during propagation. For this purpose we measured the radii of the hollow beams emerging from the metasurface and those of the incident vortex beam without the metasurface at different transmission distances. The formers minus the latter gives the radial shifts of the two split hollow beams in Fig. 6(a). It shows that the $|R\rangle$ ring shifts toward the center, whereas the $|L\rangle$ one moves outwards as propagation. The experimental results of both shifts agree well with the theoretical prediction of Eq. (8).

Third, we recorded the transverse intensities of the exit beam during propagation in order to show the occurrence of the radial SHE and the evolution of the SDS. The experimental results are presented in Fig. 6(b). As z increases, the exit beam gradually split into two hollow beams. The outer hollow beam is $|L\rangle$. Its radius becomes larger while its intensity becomes weaker as z increases. The inner beam is $|R\rangle$. Its radius and intensity almost remain constant. This is because the inward shift counteracts the divergence of the vortex beam. By applying this result, the metasurface can collimate light beams.

Finally, we studied the influence of the incident polarization on the SHE. For this purpose, we chose the incident elliptically polarized vortices with ellipticity $e = -1$, -0.18, 0, 0.18, and 1 corresponding to S, C, B, A, and N on the Poincaré sphere in Fig. 1, respectively. The five beams are then transformed by the metasurface into CV beams with radially varying polarizations, like Fig. 1(c). They thus acquire the PB geometrical phases, the spatial gradient of which leads to the SDSs into $|R\rangle$ and $|L\rangle$ rings. We measured their intensities and the results are shown in Fig. 7. It is seen that the intensities of the two rings are not necessarily equal, but depend on e. This

is because an elliptically polarized beam can be considered as a superposition of $|R\rangle$ and $|L\rangle$ with distinct amplitudes according to Eq. (3). By Eq. (4) the resulting rays, $|L\rangle$ and $|R\rangle$, possess unequal intensities. This indicates that the incident polarization affects the SDS of intensity.

IV. CONCLUSION

In summary, we identified and experimentally demonstrated another kind of SHE of light that consists of the radial SDSs of spin and intensity by a metasurface. The metasurface with periodically varying optical axes brings about a radially variant distribution of polarization, thereby endowing the incident light with an effective PB phase. Consequently, the gradient of PB phase induces a shift in the momentum space and thus gives rise to the radial SDS of light in the position space, which we call a radial SHE. Further experiments verify that the magnitude of the SDS increases with the rotation rate of optical axes and the propagation distance, which enables the SHE to be enhanced greatly for direct observation. Moreover, the SHE can be tuned by the phase and polarization of the incident light: a solid (hollow) beam with plane (spiral) phase fronts splits into one solid (hollow) beam and the other hollow beam with opposite spin; the incident polarization determines the intensities of the two separate beams. The results provide flexible and efficient ways to generate and control the SHE and CV beams [54,57]. The radial SHE could be valuable in optical manipulation and detection of particles [47,57,58], classical communication [59], and quantum communication and computation [60].

It is worth pointing out that the radial SHE of light can be extrapolated to other physical systems [4]. A radial Hall effect or SHE of electrons should be possible if applying a radially varying magnetic or electric field [61–63]. For example, we note that, most recently, Karimi *et al.* enabled an electron beam to carry a PB phase by an azimuthally varying magnetic field [64]. It follows that, if the magnetic field is made to change radially, a radial-variant PB phase and then a radial SHE of electrons could be implemented. In the future new spin-optical and spintronic devices [14,61] promise to be developed based on the radial SHE.

[1] M. Onoda, S. Murakami, and N. Nagaosa, Phys. Rev. Lett. **93**, 083901 (2004).

[2] K. Y. Bliokh and Y. P. Bliokh, Phys. Rev. Lett. **96**, 073903 (2006).

[3] O. Hosten and P. Kwiat, Science **319**, 787 (2008).

[4] K. Y. Bliokh, A. Niv, V. Kleiner, and E. Hasman, Nat. Photonics **2**, 748 (2008).

[5] K. Y. Bliokh, Y. Gorodetski, V. Kleiner, and E. Hasman, Phys. Rev. Lett. **101**, 030404 (2008).

[6] A. Aiello, N. Lindlein, C. Marquardt, and G. Leuchs, Phys. Rev. Lett. **103**, 100401 (2009).

[7] N. Shitrit, I. Bretner, Y. Gorodetski, V. Kleiner, and E. Hasman, Nano Lett. **11**, 2038 (2011).

[8] L. J. Kong, X. L. Wang, S. M. Li, Y. N. Li, J. Chen, B. Gu, and H. T. Wang, Appl. Phys. Lett. **100**, 071109 (2012).

[9] X. Yin, Z. Ye, J. Rho, Y. Wang, and X. Zhang, Science **339**, 1405 (2013).

[10] J. B. Götte, W. Löffler, and M. R. Dennis, Phys. Rev. Lett. **112**, 233901 (2014).

[11] J. Korger, A. Aiello, V. Chille, P. Banzer, C. Wittmann, N. Lindlein, C. Marquardt, and G. Leuchs, Phys. Rev. Lett. **112**, 113902 (2014).

[12] J. L. Ren, B. Wang, M. M. Pan, Y. F. Xiao, Q. H. Gong, and Y. Li, Phys. Rev. A **92**, 013839 (2015).

[13] V. S. Liberman and B. Y. Zel'dovich, Phys. Rev. A **46**, 5199 (1992).

[14] For a newest review see K. Y. Bliokh, F. J. Rodríguez-Fortuño, F. Nori, and A. V. Zayats, Nat. Photonics **9**, 796 (2015), and references therein.

[15] For a review of the SHE in inhomogeneous media, see K. Y. Bliokh, J. Opt. A **11**, 094009 (2009), and references therein.

[16] K. Y. Bliokh and Y. P. Bliokh, Phys. Rev. E **75**, 066609 (2007).

[17] V. G. Fedoseyev, J. Phys. A: Math. Gen. **21**, 2045 (1988).

[18] O. G. Rodríguez-Herrera, D. Lara, K. Y. Bliokh, E. A. Ostrovskaya, and C. Dainty, Phys. Rev. Lett. **104**, 253601 (2010).

[19] X. Zhou, Z. Xiao, H. Luo, and S. Wen, Phys. Rev. A **85**, 043809 (2012).

[20] X. Zhou, X. Ling, H. Luo, and S. Wen, Appl. Phys. Lett. **101**, 251602 (2012).

[21] A. V. Kildishev, A. Boltasseva, and V. M. Shalaev, Science **339**, 1232009 (2013).

[22] N. F. Yu and F. Capasso, Nat. Mater. **13**, 139 (2014).

[23] N. F. Yu, P. Genevet, M. A. Kats, F. Aieta, J.-P. Tetienne, F. Capasso, and Z. Gaburro, Science **334**, 333 (2011).

[24] Y. Zhao and A. Alù, Phys. Rev. B **84**, 205428 (2011).

[25] N. F. Yu, F. Aieta, P. Genevet, Mi. A. Kats, Z. Gaburro, and F. Capasso, Nano Lett. **12**, 6328 (2012).

[26] D. Lin, P. Fan, E. Hasman, and M. L. Brongersma, Science **345**, 298 (2014).

[27] N. Shitrit, I. Yulevich, E. Maguid, D. Ozeri, D. Veksler, V. Kleiner, and E. Hasman, Science **340**, 724 (2013).

[28] X. Ling, X. Zhou, X. Yi, W. Shu, Y. Liu, S. Chen, H. Luo, S. Wen and D. Fan, Light: Sci. Appl. **4**, e290 (2015).

[29] M. Beresna, M. Gecevičius, P. G. Kazansky, and T. Gertus, Appl. Phys. Lett. **98**, 201101 (2011).

[30] M. Beresna, M. Gecevičius, and P. G. Kazansky, Opt. Mater. Express **1**, 783 (2011).

[31] S. Pancharatnam, Proc. Indian Acad. Sci. Sect. A **44**, 247 (1956).

[32] M. V. Berry, J. Mod. Opt. **34**, 1401 (1987).

[33] Z. Bomzon, G. Biener, V. Kleiner, and E. Hasman, Opt. Lett. **27**, 1141 (2002).

[34] E. Hasman, Z. Bomzon, A. Niv, G. Biener, and V. Kleiner, Opt. Commun. **209**, 45 (2002).

[35] Y. Gorodetski, A. Niv, V. Kleiner, and E. Hasman, Phys. Rev. Lett. **101**, 043903 (2008).

[36] Z. Bomzon and M. Gu, Opt. Lett. **32**, 3017 (2007).

[37] G. Li, M. Kang, S. Chen, S. Zhang, E. Y. Pun, K. W. Cheah, and J. Li, Nano Lett. **13**, 4148 (2013).

[38] M. Kang, J. Chen, B. Gu, Y. Li, L. T. Vuong, and H. T. Wang, Phys. Rev. A **85**, 035801 (2012).

[39] X. Ling, X. Zhou, H. Luo, and S. Wen, Phys. Rev. A **86**, 053824 (2012).

[40] X. Ling, X. Zhou, W. Shu, H. Luo, and S. Wen, Sci. Rep. **4**, 5557 (2014).

[41] L. Marrucci, C. Manzo, and D. Paparo, Phys. Rev. Lett. **96**, 163905 (2006).

[42] M. Born and E. Wolf, *Principles of Optics* (Cambridge University Press, Cambridge, 1999).

[43] B. E. A. Saleh and M. C. Teich, *Fundamentals of Photonics* (John Wiley & Sons, New Jersey, 2007).

[44] E. J. Galvez, S. Khadka, W. H. Schubert, and S. Nomoto, Appl. Opt. **51**, 2925 (2012).

[45] F. Cardano, E. Karimi, S. Slussarenko, L. Marrucc, C. de Lisio, and E. Santamato, Appl. Opt. **51**, C1 (2012).

[46] Q. Zhan, Adv. Opt. Photonics **1**, 1 (2009).

[47] X. L. Wang, J. Chen, Y. N. Li, J. P. Ding, C. S. Guo, and H. T. Wang, Phys. Rev. Lett. **105**, 253602 (2010).

[48] B. Gu, Y. Pan, G. H. Rui, D. F. Xu, Q. W. Zhan, and Y. P. Cui, Appl. Phys. B: Lasers Opt. **117**, 915 (2014).

[49] Y. Liu, X. Ling, X. Yi, X. Zhou, S. Chen, Y. Ke, H. Luo, and S. Wen, Opt. Lett. **40**, 756 (2015).

[50] Y. Liu, X. Ling, X. Yi, X. Zhou, H. Luo, and S. Wen, Appl. Phys. Lett. **104**, 191110 (2014).

[51] F. Aieta, P. Genevet, M. A. Kats, N. F. Yu, R. Blanchard, Z. Gaburro, and F. Capasso, Nano Lett. **12**, 4932 (2012).

[52] E. Hasman, V. Kleiner, G. Biener, and A. Niv, Appl. Phys. Lett. **82**, 328 (2003).

[53] G. Yuan, E. T. F. Rogers, T. Roy, G. Adamo, Z. Shen, and I. Zheludev, Sci. Rep. **4**, 6333 (2014).

[54] B. Gu, J. L. Wu, Y. Pan, and Y. P. Cui, Opt. Express **21**, 30444 (2013).

[55] L. Allen, M. W. Beijersbergen, R. J. C. Spreeuw, and J. P. Woerdman, Phys. Rev. A **45**, 8185 (1992).

[56] A. M. Yao and M. J. Padgett, Adv. Opt. Photonics **3**, 161 (2011).

[57] F. Cardano and L. Marrucci, Nat. Photonics **9**, 776 (2015).

[58] S. Sukhov, V. Kajorndejnukul, R. R. Naraghi, and A. Dogariu, Nat. Photonics **9**, 809 (2015).

[59] G. Gibson, J. Courtial, M. J. Padgett, M. Vasnetsov, V. Pasko, S. M. Barnett, and S. Franke-Arnold, Opt. Express **12**, 5448 (2004).

[60] G. Molina-Terriza, J. P. Torres, and L. Torner, Nat. Phys. **3**, 305 (2007).

[61] S. A. Wolf, D. D. Awschalom, R. A. Buhrman, J. M. Daughton, S. von Molnár, M. L. Roukes, A. Y. Chtchelkanova, and D. M. Treger, Science **294**, 1488 (2001).

[62] C. Leyder, M. Romanelli, J. Ph. Karr, E. Giacobino, T. C. H. Liew, M. M. Glazov, A. V. Kavokin, G. Malpuech, and A. Bramati, Nat. Phys. **3**, 628 (2007).

[63] J. Sinova, S. O. Valenzuela, J. Wunderlich, C. H. Back, and T. Jungwirth, Rev. Mod. Phys. **87**, 1213 (2015).

[64] E. Karimi, L. Marrucci, V. Grillo, and E. Santamato, Phys. Rev. Lett. **108**, 044801 (2012).